

Optimal Damping Controller Design for Large-scale PV Farms to Damp the Low-frequency Oscillation

Mahdi Saadatmand*, Babak Mozafari*[‡], Gevork B. Gharehpetian**, Soodabeh Soleymani*

* Department of Electrical Engineering, Science and Research Branch, Islamic Azad University, Tehran, Iran

** Department of Electrical Engineering, Amirkabir University of Technology, Tehran, Iran

(saadatmand.ict@gmail.com, mozafari@srbiau.ac.ir, grptian@aut.ac.ir, s.soleymani@srbiau.ac.ir)

[‡]Corresponding Author; Babak Mozafari, Department of Electrical Engineering, Science and Research Branch, Islamic Azad University, Tehran, Iran, Tel: +98 21 44868401, Fax: +98 21 44868402, mozafari@srbiau.ac.ir

Received: 15.10.2019 Accepted: 17.11.2019

Abstract- With increasing the number of large-scale photovoltaic (PV) farms (LPFs) connected to the power grids in the world, some characteristics of power systems are affected. Studies show that the LPFs could have the negative effect on low-frequency oscillation (LFO) relative to their location and size. Considering that the LPFs cannot be located in ideal points and their installation location depends on geographical conditions, it is important to consider an auxiliary controller as a damping controller for them. On the other hand, the new generation of LPFs has a centralized plant controller (CPC) for voltage and power regulation at the point of common coupling (PCC); therefore, it is required to add the damping controller to the CPC. In this paper, the LFO damping by an optimal damping controller (ODC) that implemented in the CPC of LPFs is proposed. The ODC structure is a single input 2nd-order lead-lag controller. A benchmark test system for LFO studies is used to show the performance of the proposed ODC. The robustness of ODC is assessed in the different operating conditions. The simulation results demonstrate the proper function of the proposed ODC for the wide range of operating conditions.

Keywords Low-frequency oscillation (LFO), Large-scale PV farm (LPF), Optimal damping controller (ODC), Centralized plant controller (CPC), Second generation generic model (SGGM).

1. Introduction

Low-frequency oscillation (LFO) is the intrinsic event of power systems. The damping control in power systems is essential to maintain stability because the insufficient damping may give rise the risk of instability [1]. The application of power system stabilizer (PSS) for synchronous generator excitation system is the usual approach to damp the LFO. Also, some technique such as flexible AC transmission system (FACTS) has also been used for control of poorly damped LFO [2,3]. Auxiliary stabilizers applied to control the FACTS devices to increase the damping. Nowadays, increase the penetration of renewable energy power plants (REPPs) especially large-scale photovoltaic (PV) farms (LPFs) has made basic changes in power systems [4]. Currently, the LPFs are installed in many countries extensively [5]. The most of LPFs are geographically far from loads and linked to the power systems by relatively weak transmission lines. Increasing the LPFs penetration on weak transmission lines raises the probability of power system instability like as rising the possibility of LFO occurrence [5,6]. The mechanical dynamic of LPFs is

separate from the power system, but there are some mechanisms that the LPF can indirectly affect the LFO, as follows [7]:

- Replacing synchronous generators thereby affecting the LFO with LPF.
- Affecting the synchronizing forces by the Impact of LPF on the major path flows.
- Interacting the controls of LPF with the large synchronous generators damping torque.

Therefore, in a power system that includes LPF, the risk of LFO can increase [5,6]. In most cases, existing PSSs cannot have much effect. On the other hand, the impact of auxiliary devices such as energy storage systems on LFO damping has been assessed in [8]. It has been shown that the application of these devices has a positive effect on the LFO damping. Although due to their cost, the large-scale application of energy storage systems is still limited. Thus, with increasing the LPFs penetration in power systems, it is needed that these types of power plants also support the LFO damping, so designing a damping controller is essential.

However, the power system stability analysis and damping controller design require the approved dynamic model for LPFs. The latest approved model is the second generation generic model (SGGM) that developed and approved by western electricity coordinating council (WECC) and electric power research institute (EPRI) [9,10]. The SGGM is developed based on first generation generic model (FGGM) [11]. The FGGM has two modules that named PV1G and PV1E. The PV1G is for the generator converter model, and PV1E is for the electrical control model [11]. The SGGM is not very different from FGGM, except that the SGGM includes a centralized plant controller (CPC) model. The CPC model is a new module that defined in the SGGM. This module is applied for CPC modeling. In addition, the SGGM is more flexible to obtain the different control objectives to represent the different vendor equipment. Also, the most important feature of SGGM is the capability to model the future systems. It should be noted that the SGGM are still under development and testing phase [10,12] and WECC along with EPRI are working on developing and testing the LPF model. The LPFs will often employ a CPC which has the function of coordinating the response of individual PV inverters (and other active devices in the collector system, e.g. SVC or STATCOM) in order to get the required grid code response at the point of common coupling (PCC) for both voltage and reactive power regulation and primary frequency control. In [13-15], the effect of robust damping controllers designed for LPFs has been considered. In all of those researches, the FGGM and other user-written models have been used. Also, the application of their damping controllers for the LPFs that includes the CPC has not been considered.

In this paper, a supplementary optimal damping controller (ODC) is proposed for LFO damping. The structure of proposed ODC is a conventional lead-lag controller. The traditional lead-lag controller is preferred by the power system utilities because of the ease of on-line tuning and lack of assurance of the stability by some adaptive or variable structure methods [16-20]. On the other hand, it was shown that the appropriate selection of the conventional lead-lag controller parameters results in effective damping to LFOs [21]. Unfortunately, the problem of the conventional lead-lag controller design is a multimodal optimization problem (i.e., there exists more than one local optimum). Hence, the conventional optimization techniques are not suitable for such a problem. Thus, it is required that the heuristic methods, which are widely used for the global optimization problems are developed [22]. The problem of ODC design is converted to an optimization problem. So, the time-domain based objective function (OF) is defined over a wide range of operating conditions and solved by the particle swarm optimization (PSO) algorithm. To achieve the goals of this paper, the rest of the paper is organized as follows:

Section II represents the LPFs models. Section III provides the ODC model. Section IV provides the study test system and the ODC design. The controller performance evaluation and nonlinear time-domain simulations are presented in Section V. Finally; section VI draws the conclusion.

2. LPF models

The LPF includes three basic parts, the PV array, inverters and the controllers. For power system stability analysis, it is necessary to, the steady-state and dynamic models of LPF are available. So it should describe the LPFs models for steady-state and dynamic analysis.

2.1. LPF model for steady-state analysis

The PV generators within the LPF are modeled into a single generator for steady-state analysis and called the simple aggregated model [10]. This model has a MVA rating equal to the total MVA rating of individual PV generators and connected to the PCC as shown in Fig. 1.

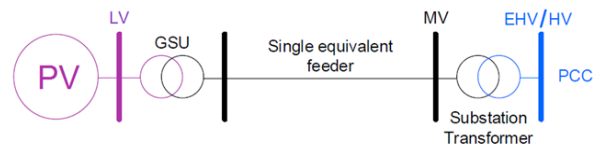


Fig. 1. The simple aggregated model for LPF.

Since the PV generators have reactive power generation/absorption capability, the LPF is considered the same as the synchronous generator for steady-state analysis, i.e. its bus is a PV or PQ bus with proper MVAr limit [11,23].

2.2. LPF model for dynamic analysis

With increasing the number of REPPs, from the beginning of 2000, there was a need for a standard, generic and flexible model for REPPs such as LPFs, for use in the software tools. Based on user experience with the FGGM for wind power plant (WPP) [24], the WECC Renewable Energy Modeling Task Force (REMTF) started the task of creating the SGGM in 2010. The WECC prepared a document for LPFs dynamic model in 2012 [25]. Later this model that is called SGGM for LPF used for power system simulations in North America in 2014 [9]. The main reason for introduced the SGGM, was to have a flexible model for the control strategies and applications. For example, in the LPFs using CPC, the implementation of the dynamic model through the FGGM is not possible, while using the SGGM, this problem is easily solved. Furthermore, the SGGM was developed based on modularity structure to allow next developments and technological compatibility [10]. The structure of the SGGM is shown in Fig.2.

The SGGM includes three modules [9,10].

- The renewable energy generator/converter (REGC_A).
- The renewable energy electrical control (REEC_B).
- The renewable energy plant control (REPC_A).

The REPC_A module has been used for CPC modeling. It should be noted that the SGGM includes a number of flags that determine the operation mode of LPF. Depending on the control strategy and PCC type, the appropriate flags can be activated. The details of the LPF operation modes have been investigated in [9].

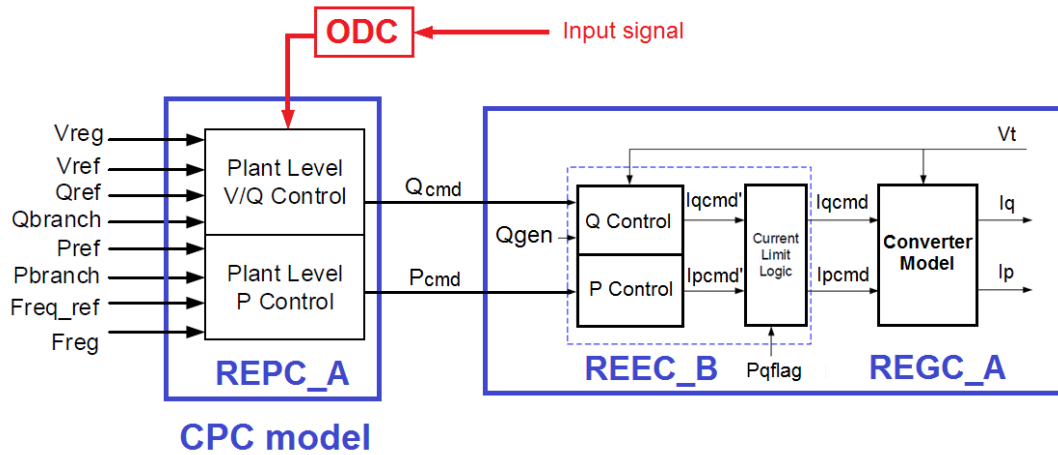


Fig. 2. Modular structure of SGGM.

3. ODC for LFO damping in LPF

In this paper, a single input 2nd-order lead-lag damping controller is proposed as an ODC for LFO damping in LPF as shown in Fig.3. The proposed controller can easily be implemented and installed. Further, the adjustment of the parameters of this controller is easily possible and the controller lacks some disadvantages of other controllers such as adaptive controller [19]. Also, it has been demonstrated that the optimal selection of this controller parameters is effective for LFO damping [26]. The ODC contains a controller gain K_{ODC} , a time constant of washout filter T_w , the time constants of 2nd-order compensator T_1, T_2, T_3 , and T_4 and a constant time delay T_m .

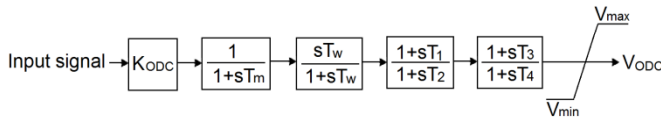


Fig. 3. 2nd-order lead-lag ODC controller.

The output signal (V_{ODC}) is subject to a limiter, V_{min} and V_{max} are minimum and maximum of V_{ODC} , and here we have 1 and -1, respectively. The ODC gain defines the amount of LFO damping and the lead-lag blocks provide the proper phase compensation of the ODC output. The selectable parameters of the proposed ODC are K_{ODC}, T_1, T_2, T_3 , and T_4 . The implementation of the proposed ODC needs the extension of the wide area measurement system (WAMS) using a communication technology [27]. The phasor measurement units (PMUs) used for measuring the considered signals. The measured signals are sent to the ODC via communication channels. Thus, it is necessary to consider the constant time delay. In this study the signal transmission delay between PMUs and ODC is considered. So a constant time delay of 100 ms is defined for ODC design [28, 29]. Also, the value of time constant of washout filter T_w is considered 10 s [28, 29].

As shown in Fig.4, two different positions are suggested for the ODC in the CPC model. Selecting each of these

positions is determined based on the operation mode of the LPF. It should be noted that these positions have been defined as auxiliary inputs in the CPC model of LPF based on SGGM for various applications [10, 12].

The position 1 in Figure 4 is recommended as the ODC placement position if the LPF operation mode is voltage control mode, or the PCC is considered as a PV bus. The position 2 is proposed as the ODC placement position when the LPF operation mode is the reactive power control mode or PCC is used as the PQ bus. In position 1, the signal type injected by ODC, is voltage type while its type is reactive power in the position 2. Furthermore, the stated modes in this section are related to the reactive power/voltage mode control while the active power/frequency control mode is not related to the placement position of the ODC. As mentioned in section 5, implementing ODC for LFO damping improves the power system response in terms of damping ratio, settling time, overshoots, and undershoots. In addition, this controller is robust to changes of power system parameters.

4. ODC designing

4.1. Test system

In this paper a two-area test system is selected as a benchmark system. This is an applied system for the study of simultaneous LFO damping [30]. The system includes four synchronous generators that presented by a sixth-order model. All synchronous generators use the simplified IEEE type ST1A excitation system. Also, the conventional type STAB1 PSS have been modeled in excitation systems of generators G2 and G4 [30]. An aggregated LPF with ODC is connected to bus 6 (PCC). This system is depicted in Fig.5. The MVA rating of the LPF is assumed 400 MVA. Also, the power rating of the generator G2 is modified from 900 MVA to 500 MVA. In addition, the system includes two load buses. Load 1 is 1767 MW and 100 MVar and Load 2 is 967 MW and 100 MVar. They are assumed as a constant power load. Other information related to the two-area test system is given in [30].

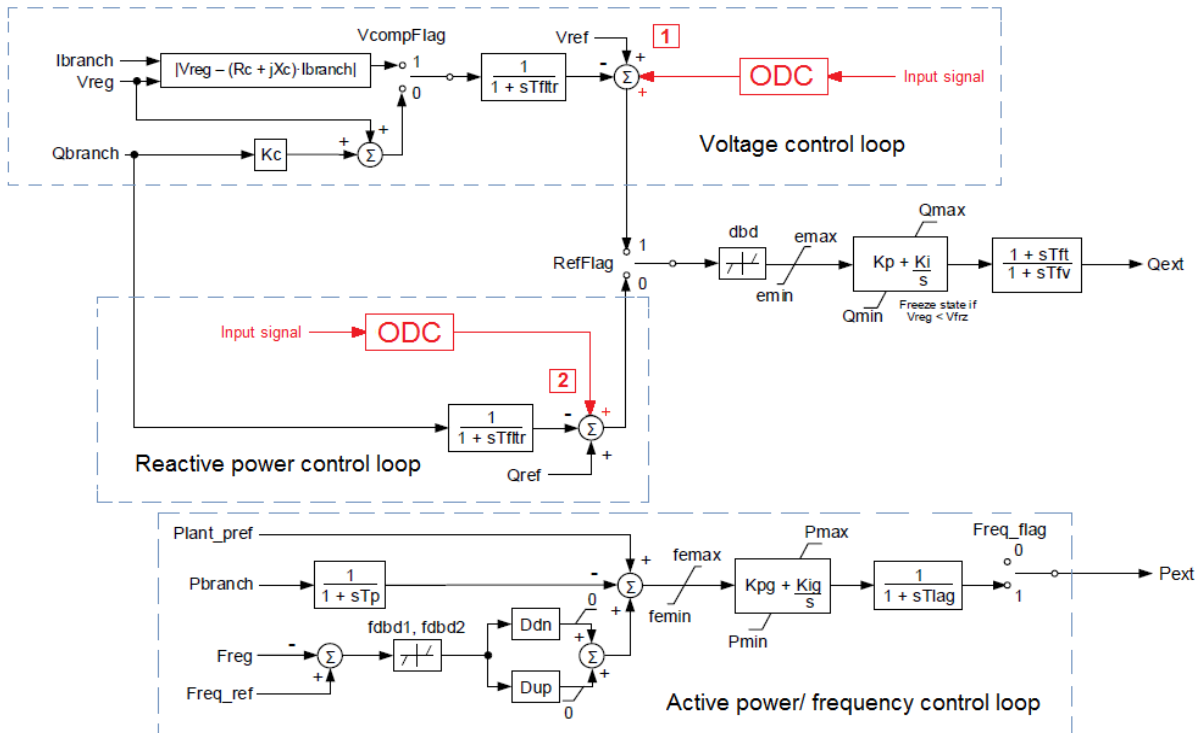


Fig. 4. CPC model of LPF based on SGGM with proposed ODC controller.

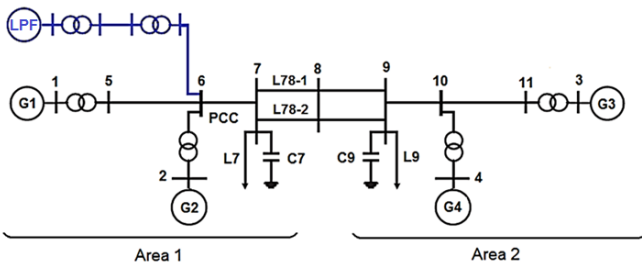


Fig. 5. Two-area test system with LPF.

As mentioned, given that the operation mode of the LPF can be voltage control or reactive power control for steady-state, the PCC bus can be modeled as a PV bus or PQ bus, respectively. In this paper, the operation mode of the LPF is considered in voltage control mode at plant level [9,10]. In this mode, the PCC is PV bus and the position 1 is considered for ODC placement. Further, the active power control mode is selected as the frequency control at plant level [9,10].

4.2. ODC design using PSO

In this subsection, the five parameters of K_{ODC} , T_1 , T_2 , T_3 and T_4 should be optimally determined for designing the ODC. Optimal tuning of this controller is challenging because there are five parameters to tune [31]. Different methods have been suggested to optimize the ODC. One of the most important of these methods is the PSO algorithm. This algorithm is a powerful method for solving optimization problems. PSO is proved to be robust in solving problems featuring nonlinearity, multiple optima, and high

dimensionality [31]. Also, other benefits of the PSO are its relative simplicity and stable convergence characteristic with good computational efficiency [31].

Since the SGGM is strongly nonlinear [9,10] and the number of optimization parameters is high, the PSO algorithm is used in this study. For each ODC, 5 parameters should be determined. The objective of the ODC is to maximize damping, minimize the overshoots, undershoots and settling times during LFO. In a wide power system, there are many generators. Thus, an OF should be formulated, which considered the impact of all generators. In this paper, the integral of the time-weighted absolute error (ITAE) performance index is used to define the OF as follows [32-35]:

$$OF = \sum_{F=1}^{N_F} \sum_{L=1}^{N_L} (ITAE)_{FL} \tag{1}$$

where, N_F is the number of fault conditions and N_L is the number of loading conditions. $ITAE$ is defined as follows [32-35]:

$$ITAE = \int_0^{t_{sim}} t \cdot \left[\sum_{G=1}^{N_G} |\Delta\omega_G(t)| \right] dt \tag{2}$$

where t indicates the time variable and t_{sim} shows the simulation time, which is 20 s in this study. Also, N_G represents the number of power system generators and $\Delta\omega_G$ represents the speed deviation of generator G . It should be noted that, $| \cdot |$ represents the absolute value.

To maintain the power system stability during the optimization process, constraints are applied to the ODC

parameters. Now, we should minimize the Eq. (1) subject to the ODC parameters constraints:

$$K_{ODC}^{min} \leq K_{ODC} \leq K_{ODC}^{max} \quad (3)$$

$$T_i^{min} \leq T_i \leq T_i^{max} \quad (4)$$

where, K_{ODC} and T_i , $i \in \{1, \dots, 4\}$ are the gain and time constants of the ODC, respectively. The ODC parameters constraints are listed in Table 1. Also, the ODC input signal is chosen as the variation of the generators speed across the two areas ($\Delta\omega$) [28, 36]. The ODC parameters are optimized by evaluating the OF at different loading and fault conditions. These conditions are given in Table 2 and 3.

Table 1. The ODC parameters constraints

Parameters	Lower bound	Upper bound
K_{ODC}	10	100
$T_i, i \in \{1, \dots, 4\}$	0.1	5

Table 2. The two fault conditions

Dynamic condition	Event
Fault condition 1	A temporary 150 ms duration three-phase short circuit at bus 8
Fault condition 2	A temporary 150 ms duration outage of tie-line L78-1

Table 3. Three loading conditions (pu)

Loading condition	L7 and L9
Case 1	Nominal loading
Case 2	90% of nominal loading
Case 3	120% of nominal loading

Various stages of the optimization algorithm are depicted in Fig.6. In order to obtain better efficiency, the number of iterations, the number of particles, the particle size, c_1 , c_2 , w_{max} , w_{min} , and c are chosen as 100, 10, 5, 2, 2, 0.9, 0.4 and 1, respectively. The PSO algorithm is run and then the optimal set of controller parameters is selected. The ODC parameters are listed in Table 4.

Table 4. Optimal values of ODC parameters

ODC Parameter	Optimal value
K_{ODC}	25.579
T_1	2.676
T_2	0.100
T_3	1.057
T_4	4.256

The convergence curve of the OF for the optimal tuning of ODC parameters is depicted in Fig.7. The best value of the OF is equal to 0.226790. It should be noted that the optimization stages are based on data exchange between MATLAB and DigSILENT PowerFactory software.

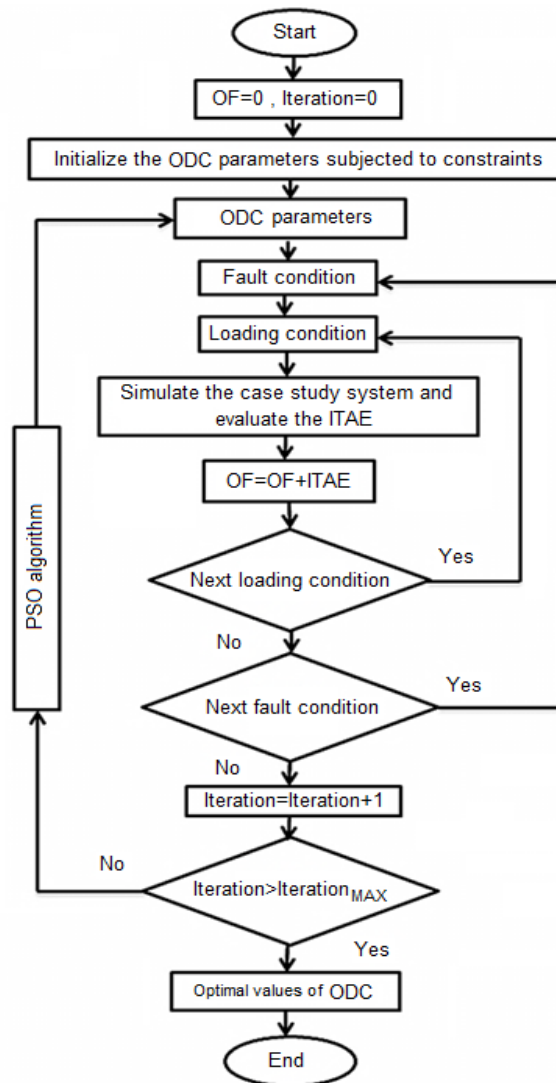


Fig. 6. Various stages of the optimization algorithm.

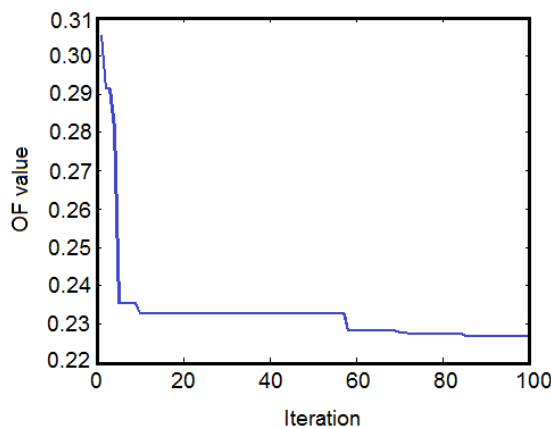


Fig. 7. Convergence curve of OF.

5. Simulation results

This section defines four states to evaluate the performance of the proposed ODC for LFO damping. The performance should be evaluated for different operating conditions [33, 36]. These states are determined in such a way that they can be different in the severity of the disturbance, although they all cause LFO in the power system. These three states are summarized as follows:

- State I: A three-phase fault at bus 8 for 180 ms.
- State II: Outage of generator *G1* at $t=1$ s for 120 ms.
- State III: Outage of load *L9* at $t=1$ s for 100 ms.

5.1. State I

In this state, a three-phase fault at bus 8 is defined to show the performance of the proposed ODC. Figure 8 demonstrates the rotor angle of generators *G1* and *G4* with and without using the ODC. This figure displays the effective performance of the proposed ODC to damp out the oscillation and stabilize the system. It is clear that the application of this controller for LPF also improves the system settling time.

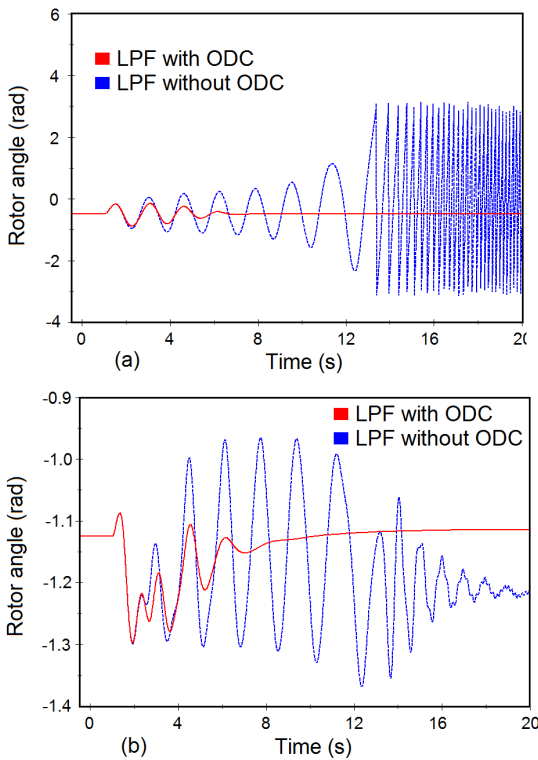


Fig. 8. Rotor angle for state I; (a) generator *G1* and (b) generator *G4*.

5.2. State II

In this state, the generator *G1* tripping at $t = 1$ s for 120 ms to shows the robustness of the proposed ODC at a large disturbance. Figure 9 shows the rotor angle of generators *G1* and *G4*. Assessment of this figure shows the suitable results of using the ODC for LFO damping.

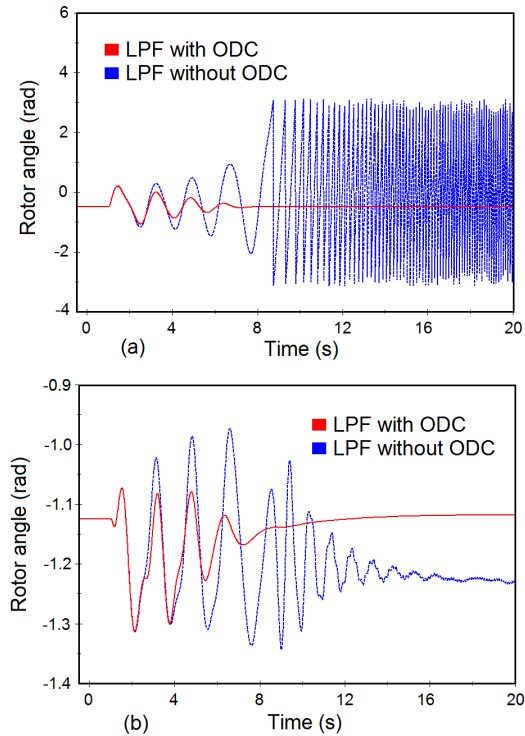


Fig. 9. Rotor angle for state II ; (a) generator *G1* and (b) generator *G4*.

5.3. State III

The robustness of the proposed ODC is tested after load *L9* is opening at $t = 1$ s for 100 ms. Figure 10 represents the rotor angle of generators *G1* and *G4*.

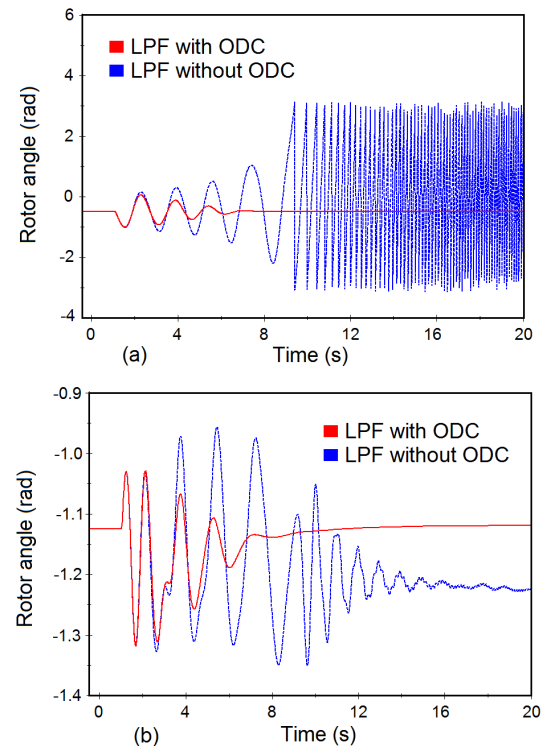


Fig. 10. Rotor angle for state III; (a) generator *G1* and (b) generator *G4*.

Also, Fig. 11 shows the tie-line (L78-2) active power swing for three states, with and without using the ODC.

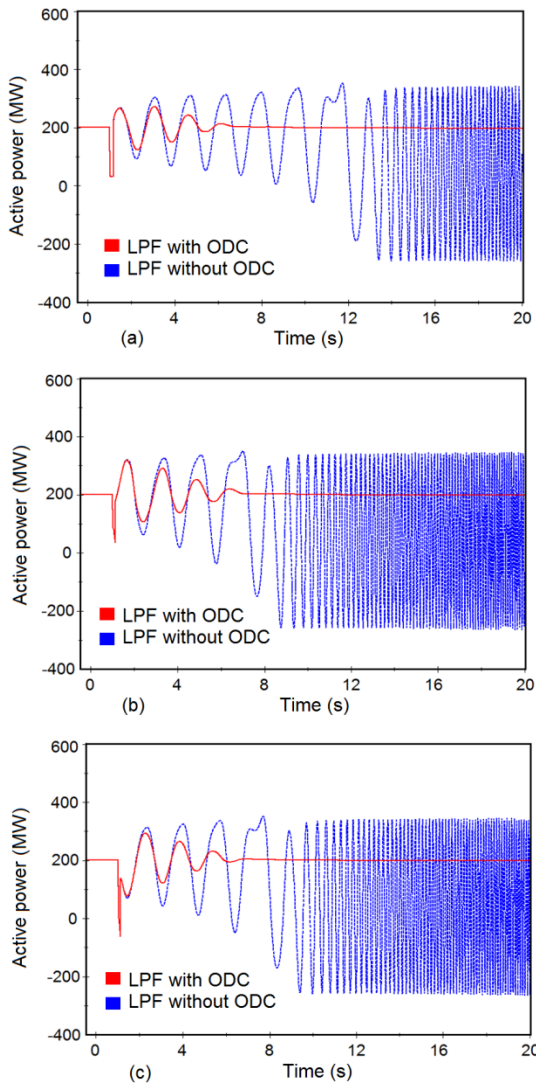


Fig. 11. Active power of tie-line L78-2; (a) state I (b), state II and (c) state III.

All results represent that although the proposed ODC is designed for specific state, however, it can also damp the LFO under other disturbances introduced by states I to III. Another serious contingency is different loading conditions of the power systems. So it is needed to evaluate the performance of the proposed ODC under different loading conditions. In this study to evaluate the desired performance of the proposed ODC, the *ITAE* index is used [35]. Here each of above mentioned states is investigated under three loading conditions as listed in Table.3. It should be noted that the lower value of this index indicates the better LFO damping. The numerical results of different loading conditions are shown in Fig.12.

The simulation results show that the application of the ODC for the LPF improves the damping ratio and settling time in all states. Also, the ODC is more effective in terms of reducing the overshoot and undershoot and.

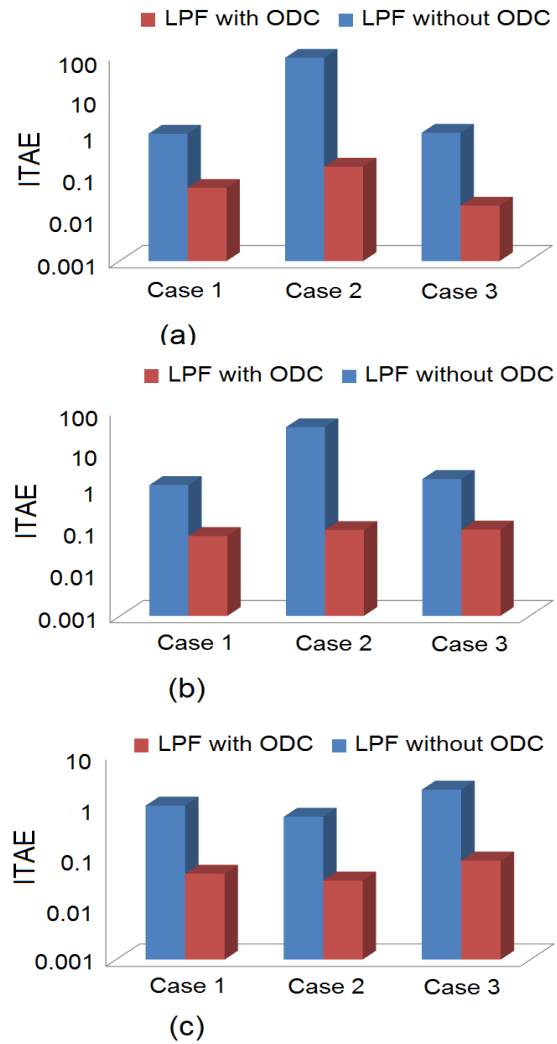


Fig. 12. *ITAE* index; (a) State I, (b) State II and (c) State III.

6. Conclusion

In this paper, the possibility of using the ODC for LPF, to effectively LFO damping has been investigated. For this purpose the SGM has been selected as the LPF dynamic model, and the proposed ODC has been implemented in the CPC module as an auxiliary controller. The problem of selecting the ODC parameters to increase the LFO damping has been successfully solved by the PSO algorithm. The effectiveness of the ODC has been evaluated on the benchmark test system under different loading and fault conditions. The simulation results show its ability to provide the suitable LFO damping. It should be noted that the proposed ODC does not have any adverse effect on other system oscillations.

References

[1] G. Rogers, Power System Oscillations, New York: Springer Science & Business Media, 2000.
 [2] B. Pal, B. Chaudhuri, Robust Control in Power Systems, New York: Springer Science & Business Media, 2005.

- [3] J. Deng, C. Li, X.P. Zhang, "Coordinated design of multiple robust FACTS damping controllers: A BMI-based sequential approach with multi-model systems", *IEEE Transactions on Power Systems*, vol. 30, pp. 3150-3159, January 2015.
- [4] P. Cherukad, M. Lydia, "A Comprehensive Overview on PV based Hybrid Energy systems", *International Journal of Renewable Energy Research (IJRER)*, vol. 9, pp. 1241-1248, September 2019.
- [5] R. Shah, N. Mithulananthan, R.C. Bansal, V.K. Ramachandaramurthy, "A review of key power system stability challenges for large-scale PV integration", *Renewable and Sustainable Energy Reviews*, vol. 41, pp. 1423-1436, January 2015.
- [6] S. Eftekharijad, V. Vittal, G.T. Heydt, B. Keel, J. Loehr, "Impact of increased penetration of photovoltaic generation on power systems", *IEEE Transactions on Power Systems*, vol. 28, pp. 893-901, October 2012.
- [7] J. Quintero, V. Vittal, G.T. Heydt, H. Zhang, "The impact of increased penetration of converter control-based generators on power system modes of oscillation", *IEEE Transactions on Power Systems*, vol.29, pp. 2248-2256, February 2014.
- [8] R. Shah, N. Mithulananthan, R.C. Bansal, "Damping performance analysis of battery energy storage system, ultracapacitor and shunt capacitor with large-scale photovoltaic plants", *Applied Energy*, vol. 96, pp. 235-244, August 2012.
- [9] WECC Renewable Energy Modeling Task Force. WECC PV power plant dynamic modeling guide, Western Electricity Coordinating Council, 2014.
- [10] Pourbeik P. Model user guide for generic renewable energy system models, Electric Power Research Institute, 2015.
- [11] K. Clark, N.W. Miller, R. Walling, R. Modeling of GE solar photovoltaic plants for grid studies, version 1, GE International Inc, 2009.
- [12] P. Pourbeik, J.J. Sanchez-Gasca, J. Senthil, J.D. Weber, P.S. Zadehkhosht, Y. Kazachkov, S. Tacke, J. Wen, A. Ellis, "Generic Dynamic Models for Modeling Wind Power Plants and Other Renewable Technologies in Large-Scale Power System Studies", *IEEE Transactions on Energy Conversion*, vol. 32, pp. 1108-1116, December 2016.
- [13] R. Shah, N. Mithulananthan, K.Y. Lee, "Large-scale PV plant with a robust controller considering power oscillation damping", *IEEE Transactions on Energy Conversion*, vol. 28, pp. 106-116, December 2012.
- [14] L. Zhou, X. Yu, B. Li, C. Zheng, J. Liu, Q. Liu, K. Guo, "Damping Inter-Area Oscillations With Large-Scale PV Plant by Modified Multiple-Model Adaptive Control Strategy", *IEEE Transactions on Sustainable Energy*, vol. 8, pp. 1629-1636, April 2017.
- [15] Y. Shen, W. Yao, J. Wen, H. He, "Adaptive wide-area power oscillation damper design for photovoltaic plant considering delay compensation", *IET Generation, Transmission & Distribution*, vol. 11, pp. 4511-4519, April 2017.
- [16] D. Rekioua, T. Rekioua, Y. Soufi, "Control of a grid connected photovoltaic system", *International Conference on Renewable Energy Research and Applications (ICRERA)*, pp. 1382-1387, November 2015.
- [17] J. Zhang, D. Guo, F. Wang, Y. Zuo, H. Zhang, "Control strategy of interlinking converter in hybrid AC/DC microgrid", *International Conference on Renewable Energy Research and Applications (ICRERA)*, pp. 97-102, October 2013.
- [18] K.D. Mercado, J. Jimenez, M.C. Quintero, "Hybrid renewable energy system based on intelligent optimization techniques", *International Conference on Renewable Energy Research and Applications (ICRERA)*, pp. 661-666, November 2016.
- [19] S. Panda, N.P. Padhy, "Comparison of particle swarm optimization and genetic algorithm for FACTS-based controller design", *Applied Soft Computing*, vol. 8, pp.1418-1427. September 2008.
- [20] H. Shayeghi, H.A. Shayanfar, S. Jalilzadeh, A. Safari, "A PSO based unified power flow controller for damping of power system oscillations", *Energy Conversion and Management*, vol. 50, pp. 2583-2592. October 2009.
- [21] M. A. Abido, "Pole placement technique for PSS and TCSC based stabilizer design using simulated annealing", *International Journal of Electrical Power & Energy systems*, vol. 22, pp. 543-554. November 2000.
- [22] T. GT, T. SK, "Refinement of conventional PSS design in multimachine system by modal analysis", *IEEE Transactions on power systems*, vol. 8, pp. 598-605, May 1993.
- [23] F. Delfino, R. Procopio, M. Rossi, G. Ronda, "Integration of large-size photovoltaic systems into the distribution grids: a P-Q chart approach to assess reactive support capability", *IET Renewable Power Generation*, vol. 4, pp. 329-340, July 2010.
- [24] A. Ellis, Y. Kazachkov, E. Muljadi, P. Pourbeik, J.J. Sanchez-Gasca, "Description and technical specifications for generic WTG models", *IEEE/PES Power Systems Conference and Exposition, Phoenix*, pp. 1-8, 20-23 March 2011.
- [25] WECC Renewable Energy Modeling Task Force. WECC solar PV dynamic model specification, Western Electricity Coordinating Council, 2012.
- [26] H. Shayeghi, H.A. Shayanfar, A. Safari, R. Aghmasheh, "A robust PSSs design using PSO in a multi-machine environment", *Energy Conversion and Management*, vol. 51, pp. 696-702. April 2010.
- [27] B. Ramezy, M. Saadatmand, B. Mozafari, "Review of Communication Technologies for Smart Grid applications", *The National Conference on: New Approaches in Power Industry, Tehran*, October 2017.

- [28] D. Cai, Wide Area Monitoring, Protection and Control in the Future Great Britain Power System, PhD Dissertation, Manchester: The University of Manchester, 2012.
- [29] A.S. Lunardi, J.S. Lucena, I.R. Casella, C.E. Capovilla, A.J. Sguarezi Filho, "Wireless communication applied in a grid tie converter control for renewable sources", IEEE 6th International Conference on Renewable Energy Research and Applications (ICRERA), pp. 552-555, November 2017.
- [30] P. Kundur, N.J. Balu, M.G. Lauby, Power system stability and control, New York: McGraw-Hill, 1994.
- [31] M. Zamani, M. Karimi-Ghartemani, N. Sadati, M. Parniani, "Design of a fractional order PID controller for an AVR using particle swarm optimization", Control Engineering Practice, vol. 17, pp. 1380-1387, December 2009.
- [32] E. Mostafa, N.K. Bahgaat, "A Comparison Between Using A Firefly Algorithm and A Modified PSO Technique for Stability Analysis of a PV System Connected to Grid", International Journal of Smart Grid-ijSmartGrid. Vol. 1, pp. 1-8, December 2017.
- [33] T.K. Das, G.K. Venayagamoorthy, UO Aliyu, "Bio-inspired algorithms for the design of multiple optimal power system stabilizers: SPPSO and BFA", IEEE Transactions on Industry Applications, vol. 44, pp. 1445-1457, September 2008.
- [34] H. Shayeghi, A. Safari, H.A. Shayanfar, "PSS and TCSC damping controller coordinated design using PSO in multi machine power system", Energy Conversion and Management, vol. 51, pp. 2930-2937, December 2010.
- [35] Y. Nie, Y. Zhang, Y. Zhao Y, B. Fang B, L. Zhang, "Wide-area optimal damping control for power systems based on the ITAE criterion", International Journal of Electrical Power & Energy Systems, vol. 106, pp. 192-200, March 2019.
- [36] F.M. Gonzalez-Longatt, J.L. Rueda, PowerFactory Applications for Power System Analysis, New York: Springer, 2014, ch.13.